

Usage of coot optimization-based random forests analysis for determining the shallow foundation settlement

Yi Han¹, Xingliang Jiang^{*2}, Ye Wang¹ and Hui Wang³

¹School of Architecture, Anhui Science and Technology University, Bengbu, Anhui, 233100, China

²CCCC Water Transportation Consultants Co., Ltd., Beijing 100007, China

³Department of Civil Engineering, Tongji University, Shanghai 200092, China

(Received October 13, 2022, Revised January 8, 2023, Accepted January 13, 2023)

Abstract. Settlement estimation in cohesion materials is a crucial topic to tackle because of the complexity of the cohesion soil texture, which could be solved roughly by substituted solutions. The goal of this research was to implement recently developed machine learning features as effective methods to predict settlement (S_m) of shallow foundations over cohesion soil properties. These models include hybridized support vector regression (SVR), random forests (RF), and coot optimization algorithm (COM), and black widow optimization algorithm (BWOA). The results indicate that all created systems accurately simulated the S_m , with an R^2 of better than 0.979 and 0.9765 for the train and test data phases, respectively. This indicates extraordinary efficiency and a good correlation between the experimental and simulated S_m . The model's results outperformed those of ANFIS – PSO, and COM – RF findings were much outstanding to those of the literature. By analyzing established designs utilizing different analysis aspects, such as various error criteria, Taylor diagrams, uncertainty analyses, and error distribution, it was feasible to arrive at the final result that the recommended COM – RF was the outperformed approach in the forecasting process of S_m of shallow foundation, while other techniques were also reliable.

Keywords: forecasting; optimization algorithms; random forests; settlement; shallow foundation; support vector regression

1. Introduction

The varied and complicated character of soil makes it an ideal medium. Owing to the intricacy and ambiguity of the situation, variations in the soil's properties are unavoidable. The large inherent uncertainty in the soil attributes relies on the site situation because of the inherent randomness of the soil creation mechanism. Therefore, all of the changes in the soil's qualities must be taken into account before building any construction on it (Sarkhani Benemaran *et al.* 2022, Esmacili-Falak *et al.* 2018). Common constructions that are built on the earth's surface and through which the weight of other structures is transferred to the ground are shallow foundations. The soil carrying capacity and foundation settling are the two key factors that influence shallow foundation design. In addition, settlement instead of bearing capacity governs the design of shallow foundations (Schmertmann 1970).

Empirical equations according to permitted bearing capacity and settlement requirements are often utilized in the traditional design of shallow foundations built on cohesive soil (Esmacili-Choobar *et al.* 2013). The final bearing capacity must be reduced by the factor of safety to get the allowed bearing capacity of the shallow foundation (Sarkhani Benemaran *et al.* 2020). Additionally, the factor of safety technique is often employed to determine footing

settlement since it is straightforward and directly related to the settlement. Nevertheless, it disregards the unknowns around the factors influencing the soil qualities (Duncan 2000, Peschl *et al.* 2002, Wang *et al.* 2020, Whitman 2000, Zhang and Goh 2012). Phoon demonstrated that the variability in test results is caused by both testing errors and variations in the soil deposits (Phoon 2002). When input variables are treated as random variables, and the impacts of the input data on outcomes are examined by various models, reliability analysis has been conducted to account for changes in soil qualities. Many academics have conducted their study utilizing the probabilistic method, developing models employing probabilistic ideas for the estimation of the total settlement utilizing either conventional penetration test data or consolidation test data (Krizek *et al.* 1978). A probabilistic technique was then suggested for the use of an efficient frictional angle solution for the final bearing capacity for a shallow foundation footing on cohesionless soil (Cherubini 2000). In order to provide a probabilistic remedy to evaluate the bearing capacity of a shallow foundation placed on cohesionless soil, it was utilized two variables (effective frictional angle and soil unit weight). This study also demonstrated that unit weight variation has a significant impact on the bearing capacity of shallow foundations (Easa 1992).

Numerous scholars used various techniques to perform reliability analysis. Various studies using experimental datasets have been developed for solving different problems of engineering (Esmacili-Falak *et al.* 2019, Zhu, *et al.* 2022, Aghayari Hir *et al.* 2022, Shi *et al.* 2023, Yuan *et al.* 2022, Yang *et al.* 2022). In order to calculate settlement and

*Corresponding author, BSc.
E-mail: ranmingzh@163.com

bearing capacity, Babu and Srivastava employed the response surface method (*RSM*) to create an approximation polynomial function utilizing a valid range of soil properties as input (Babu and Srivastava 2007). Multi-layer perceptron (*MLP*) and B-spline Neuro-fuzzy networks are two modeling types that Shahin *et al.* developed and implemented for predicting shallow foundation settling on granular soil (Shahin *et al.* 2003b). Karimi investigated the behavior of a valley that had been filled with silt using neuro-fuzzy systems (Karimi 2003). Hasanipناه *et al.* employed the particle swarm optimization-artificial neural network (*PSO – ANN*) approach to forecast the maximum surface settlement brought on by tunneling, demonstrating that this model is more accurate than *ANN* in predicting maximum surface settlement (Hasanipناه *et al.* 2016). According to Tarawneh, *ANN* has great accuracy ($R^2 = 0.95$, $MAE = 2.88$) when predicting the N_{60} -value using *CPT* data and a back propagation neural network (*BPNN*) (Tarawneh 2017). The shear strength of squat reinforced concrete walls was predicted by Chen *et al.* using the *PSO – ANN* modeling approach, and the algorithm demonstrated great forecasting reliability (Chen *et al.* 2018).

The geotechnical literature describes a number of theoretical and experimental techniques for predicting the settling of shallow foundations on various kinds of soil (Bungenstab and Bicalho 2016, Fattah *et al.* 2013, Lehane and Cosgrove 2000 Maugeri *et al.* 1998, Tarawneh *et al.* 2013, Tsai *et al.* 2013). As shown in Fig. 1, a number of factors, including net applied pressure, the soil's Poisson's ratio, its average modulus of elasticity, and the dimensions of the foundation, are often taken into account when determining the amount of soil settlement. Due to the relationship with various variations, the settlement behavior is a very challenging geotechnical engineering issue.

Many methodologies for settlement forecasting have focused on the correlations between in situ investigations, such as the standard penetration test (*SPT*) (Standard 2008), cone penetration test (*CPT*) (Robertson and Cabal 2014),

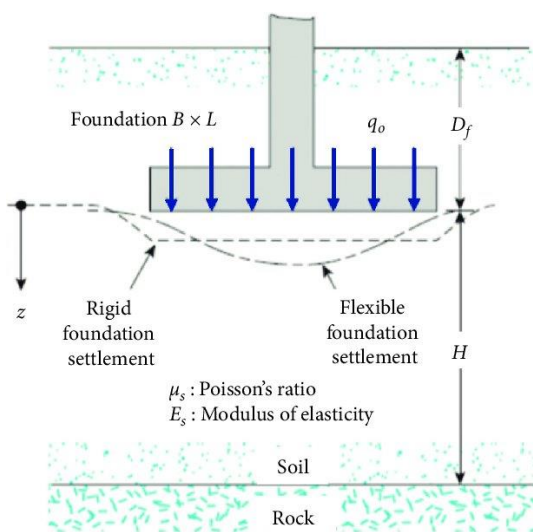


Fig. 1 Some of the related variables on foundation-soil settlement

dilatometer test (Mayne 2007), plate load test (Consoli *et al.* 1998), and screw plate load test, because of the difficulty in acquiring specimens for cohesionless soils. Most of the solutions that are now in use simplify the issue by making a number of assumptions about the variables that influence settlement. These approaches, which range from being essentially empirical to using complicated nonlinear finite elements, are thus unable to provide a reliable and precise settlement forecast (Jebur *et al.* 2018). Numerous comparison research employing machine learning models across the literature showed conflicting settlement forecast magnitudes. Therefore, the motivation for geotechnical scientists to seek and examine is always a trustworthy alternative model (Mohamed A Shahin *et al.* 2001). A new age of modeling approaches for many engineering applications was shown by machine learning frameworks (Al-Musawi *et al.* 2020, Alwanas *et al.* 2019, Ashrafian *et al.* 2020, Naderpour *et al.* 2019, 2020, Sharafati *et al.* 2021, Yaseen *et al.* 2018), especially in geotechnical problems (Alzabeebee *et al.* 2022, Kamran *et al.* 2022, Kidega *et al.* 2022; Mahmoodzadeh *et al.*, 2022, Mirzaeiabdolyousefi *et al.* 2022). *ANN* models for settlement assessment have been used in this sector for almost three decades (Chen *et al.* 2019, Moayedi and Jahed Armaghani 2018, Shi *et al.* 1998, Sivakugan *et al.* 1998, Teh *et al.* 1997). Several implementations employing various *AI* models, such as gene expression programming (Armaghani *et al.* 2018, Soleimani *et al.* 2018), support vector machines (Samui 2008), least square support vector machines (Samui and Sitharam 2008), neuro-fuzzy networks (Luo *et al.* 2018, Shahin *et al.* 2003a), and recently Random Forests (*RF*) analysis (Chen *et al.* 2022, Ghosh *et al.* 2022), followed this during the course of the previous 20 years. Nevertheless, the primary issue of standalone *AI* techniques is the internal hyperparameter adjustment; as a result, the era of modeling techniques for simulating complex engineering problems now involves combining these models with optimization methods to create what is known as a hybrid model (Benemaran and Esmacili-Falak 2020a, Kar 2016, Pham *et al.* 2019, Sarkhani Benemaran *et al.* 2022, Yaseen *et al.* 2018). The solar radiation and wind speed were predicted using combined *RF* with coot optimization algorithm (*COM*) and particle swarm optimization (*PSO*) (Islam *et al.* 2021), daily reference evapotranspiration was estimated by hybrid *COOT – ANN* (Mirzania *et al.* 2022), seasonal maximum wave height for unevenly spaced time series was forecasted by hybridized adaptive neuro fuzzy inference system (*ANFIS*) and support vector regression (*SVR*) with black widow optimization algorithm (*BWOA*), and *PSO* (Memar *et al.* 2021), dissolved oxygen concentration predictions for running waters was performed by hybrid *BWOA – SVR* method (Dehghani *et al.* 2022), *BWO – SVR* analysis was developed for simulating the precipitation runoff process (Dehghani *et al.* 2022), so on.

In the present study, the prediction of shallow foundation settlement applying data mining methods was considered as the principal goal in order to decrease the supplied works and costs. Among various machine learning methods employed for estimation purposes, *SVR* and *RF* were considered because of their applicability and

Table 1 Statistical characteristics of the variables to create the analysis

Data	Index							
	Max.	Min.	St. d.	Avg.	median	Skew.	Var.	Kur.
Inputs								
<i>Footing width (B) (m)</i>								
Train	60	0.8	9.0428	7.99	4.55	2.4351	81.771	7.867
Test	55	0.9	12.587	11.15	5.1	1.647	158.45	2.564
<i>Footing net applied pressure (q) (kpa)</i>								
Train	697	18.32	123.401	186.13	151.6	2.0062	15227.81	4.555
Test	584	25	121.4229	190.01	162	1.41	14743.52	2.619
<i>The average SPT blow count (N)</i>								
Train	60	4	13.09	24.58	20	0.847	171.3	0.158
Test	60	4	14.66	24.55	20	0.672	215.013	-0.304
<i>Footing embedment ration (D_f/H)</i>								
Train	3.44	0	0.5286	0.51	0.47	2.5254	0.2794	8.7215
Test	3	0	0.70183	0.61	0.4	1.9967	0.4925	4.184
<i>Footing geometry (L/B)</i>								
Train	10.6	1	1.731	2.22	1.6	2.005	2.997	4.623
Test	9.9	1	1.9676	2.11	1.1	2.588	3.871	6.755
Output								
<i>Average settlement (S_m) (mm)</i>								
Train	121	0.6	25.4178	19.43	11	2.435	646.06	5.0631
Test	120	1.3	29.456	23.51	10.9	2.05446	867.656	3.681

powerfulness. Within the *SVR* and *RF* models exist some determinative parameters that control the performance and accuracy of final outputs. These determinative variables could be specified by trial and test methods or hybridizing with optimization algorithms. In this study, two newly developed optimization algorithms named *COM* and *BWOA* were considered for this purpose. On the basis of shallow foundation settlement, which was taken into consideration throughout the literature review, the viability of the examined hybridization models was validated. The key benefit of the recommended networks is their ability to reproduce the nonlinearity relationship between the inputs (related qualities) and the outputs (target parameters) without the need for a predetermined formulation.

2. Dataset explanation

As previously indicated, a variety of hybrid techniques are used to create prediction models that predict settlements of shallow footings (S_m). In order to do this, a complete collection of in-situ measurements of elastic foundation settlement, including 190 data rows, was gathered from the literature (Shahin 2003). The database includes the necessary data on the footing and soil, which were measured during in-situ settlements of shallow footings under various circumstances. The requirements listed include a wide variety of adjustments to the footing's geometric specifications as well as soil classification and

soil properties. It should be noted that the reliability of the built algorithms will rise with broad data collection. The collected database was divided into two sections, the training component and the testing portion, with a percentage of $\frac{3}{4}$ (142) and $\frac{1}{4}$ (47), respectively, in accordance with the literature and research (Benemaran and Esmacili-Falak 2020b, Sarkhani Benemaran *et al.* 2022). Significant variables were chosen as input data (Shahin 2003), such as footing width (B) (m), footing net applied pressure (q) (kpa), the average *SPT* blow count (N), footing embedment ration (D_f/H), and footing geometry (L/B) in order to estimate S_m . The statistical characteristics of the gathered collection for components are listed in Table 1. The distribution of each input parameter was presented in Fig. 2 with the intention of highlighting the dataset's breadth.

The Pearson Correlation Coefficient (*PCC*) was used by the authors to describe the relationship between two variables in the dataset that were computed using Eq (1).

$$R_{X,Y} = \frac{cov(X,Y)}{\sigma_X \sigma_Y} \quad (1)$$

$cov(X,Y)$: Covariance between X and Y

σ_X : The standard deviation of X

σ_Y : The standard deviation of Y

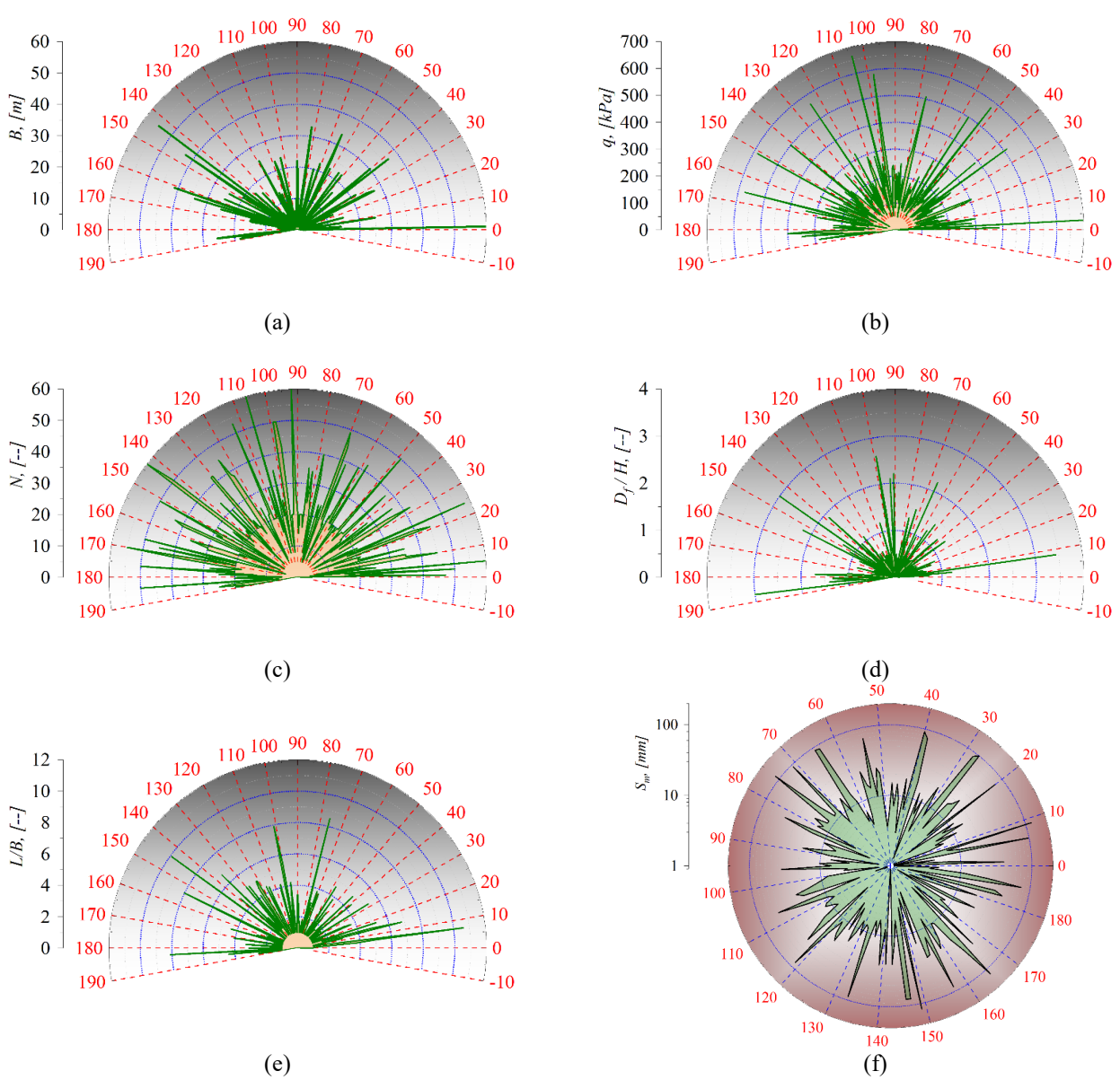


Fig. 2 Distribution of input variables, (a)-(e) inputs, (f) output

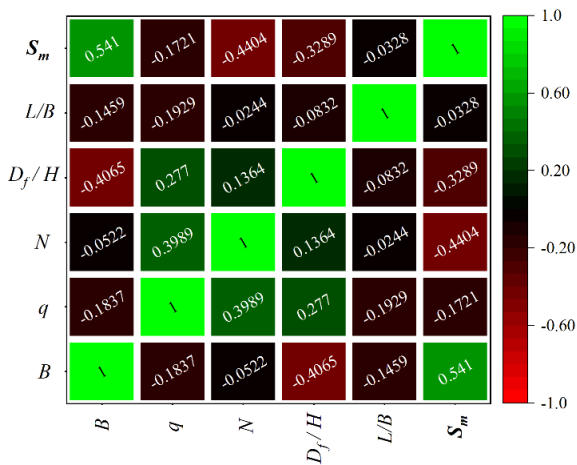


Fig. 3 Pearson Correlation Coefficient (PCC) between variables

The values of PCCs between input parameters and outcome are displayed in Fig. 3. A sign of inadequate methods might be completely big positive or negative PCC, which makes it impossible to determine how the explanatory variables have influenced the conclusions in the model. Since a significant number of PCCs were below -0.4065, these items are probably not the root cause of multicollinearity problems (Farrar and Glauber 1967). As it is clear, high correlations between variables exist, such as between B and S_m as positive correlation at 0.541. Along with this, the highest negative correlations belonged to between N and S_m by -0.754.

3. Applied analysis and optimizers

3.1 Optimization algorithms



Fig. 4 (a) Disordered stage and (b) Synchronized stage (Trenchard 2012)



Fig. 5 Moving the coots' chain on the water (Trenchard 2012)

3.1.1 COOT optimization method (COM)

The Coot optimization algorithm is constructed on various flow behaviors of coot groups that are moving on the water surface (Figs. 4 and 5). Small water birds called coots move mostly in the direction of food or a particular site to reach their target. They engage in a variety of group activities on the water's surface. As a result, as these birds travel on the water's surface, four various sorts of motions result, including chain movement, leader movement, random movement, and position adjustment in accordance with the leader (Naruei and Keynia 2021). According to (Naruei and Keynia 2021), Eqs. (2) and (3) implement the unique method of the COM.

The population's random initialization is constructed using Eq. (2)

$$cootpos(i) = rand(1, d) \times (ub - lb) + lb \quad (2)$$

The coot position is represented by $cootpos(i)$, the number of variables or dimensions of the problem is represented by d , and the upper and lower bounds of the search space are represented by ub and lb , respectively. The ub and lb in Eq. (8) may vary from those mentioned in Eq. (7).

$$lb = [lb_1, lb_2, \dots, lb_a], ub = [ub_1, ub_2, \dots, ub_a] \quad (3)$$

Following the random initialization of the population and the location of each coot, the objective function is used

to address the problem of the fitness of computed data to observed data. The number of coots needed to do that when group leaders were picked at random is equal to NL . The coots' four motions on the water's surface will thus be put into practice.

Random movement

The search space for the coots' random location, which is being recommended as a search space, is constrained by Eq. (4) (Fig. 6)

$$Q(i) = rand(1, d) \times (ub - lb) + lb \quad (4)$$

The coots' mobility allows them to investigate various regions of the search space, which increases the likelihood that the algorithm may get stuck at a local ideal. Since the algorithm in this instance moved away from this local, Eq. (5) will be utilized to determine the coot's new location.

$$cootpos(i) = cootpos(i) + A \times R_2 \times (Q - cootpos(i)) \quad (5)$$

Where A is determined using Eq. (6), and R_2 represents a random integer in the range $[0, 1]$

$$A = 1 - L \times (1/Iter) \quad (6)$$

$Iter$ indicates the maximum number of iterations, whereas L denotes the current iteration.

Chain movement

The average location and the distance vector are the two methods for determining the chain movement for two coots (Fig. 7). By using the two routes, one coot is going in a direction that is equal to the distance in half between the two coots. In this investigation, the coot's new location was calculated using the average mathematical position and is shown in Eq. (7)

$$cootpos(i) = 0.5 \times (cootpos(i - 1) + cootpos(i)) \quad (7)$$

where $cootpos(i - 1)$ denotes the second coot's placement.

Adjustment of the position

The coot advances in this manner toward the group leader, opening up several opportunities for each coot to follow various leaders in various places (Fig. 8). As a result, it is challenging to predict how one coot would move in relation to numerous leaders. In order to tackle this difficulty, an average position for multiple leaders must be taken into account. Where $Iter$ denotes the maximum iteration, and L denotes the current iteration. In conclusion, as shown by Algorithm 1, the COM has implemented the general issue. As a result, each coot may adjust its location in accordance with the average placement (Fig. 9), and the leader could be chosen using Eq. (8).

$$K = 1 + (i \text{ MOD } NL) \quad (8)$$

Based on Eq. (8), the current coot is shown as i , and the number of leaders is depicted as NL where K is indicated as the number of the leader index. $Coot(i)$ must thus alter its location in accordance with the leader's K . The following location of the $coot(i)$ may be computed depending on the chosen leader, and Eq. (9) will then be tried to apply:

$$cootpos(i) = leaderpos(k) + 2 \times R_1 \times \cos(2R\pi) \times (leaderpos(k) - cootpos(i)) \quad (9)$$

$cootpos(i)$: Current location of the coot

$leaderpos(k)$: The chosen leader's location

R_1 , and R : A random number between the interval $[0, 1]$ and $[-1, 1]$

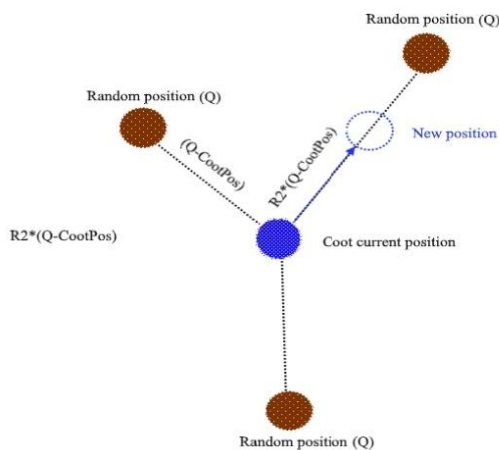


Fig. 6 Coots' random movement (Naruei and Keynia 2021)

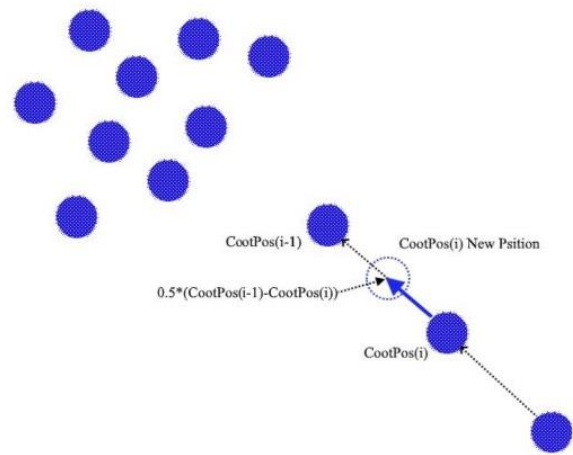


Fig. 7 Coots' chain movement (Naruei and Keynia 2021)

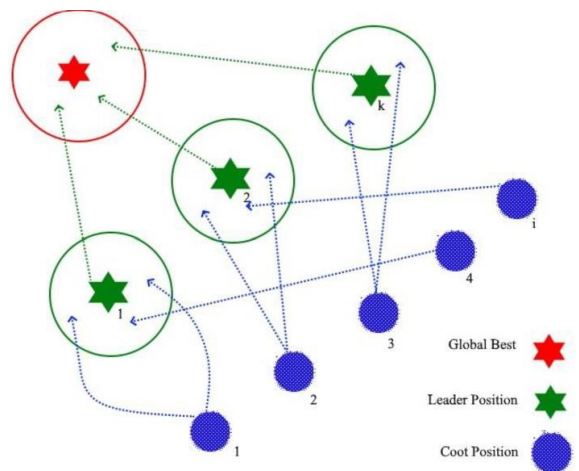


Fig. 8 Coots' leader selection mechanism (Naruei and Keynia 2021)

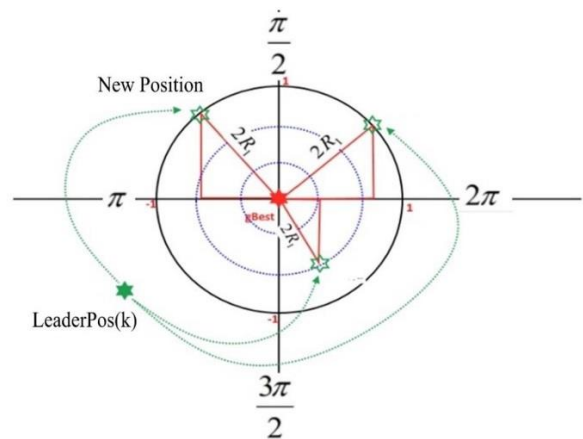


Fig. 9 Readjust the leaders' locations relative to the proper location (Naruei and Keynia 2021)

The leading movement to the optimal area

Coots in this movement must adjust their locations to the primary location that the leaders are in, and leaders in this movement must also move about to find the best location from which the coots will follow them. In order to determine where leaders should be most effective, Eq. (10) will be used

Algorithm 1 The pseudo-code of COM (Naruei and Keynia 2021)

```

1. Initialize the first population of coots randomly by Eqs. (2) and (3)
2. Initialize the parameters of P=0.5, NL (number of leaders), NCOOT (Number of coots)
3. NCOOT = Npop - NL
4. Random selection of leaders from the coots
5. Calculate the fitness of coots and leaders
6. Find the best coot or leader as the Global optimum (gBest)
7. while the end criterion is not satisfied
8. Calculate A and B parameters by Eqs. (6) and (11)
9.   if rand < P
10.    R, R1, and R3 are random vectors along the dimensions of the problem
11.    else
12.    R, R1, and R3 are random number
13.    end
14.    for i = 1 to the number of coots
15.    Calculate the parameter of k by Eq. (8)
16.    if rand > 0.5
17.    Update the position of the coot by Eq. (9)
18.    else
19.    if rand < 0.5 i ≅ 1
20.    Update the position of the coot by Eq. (7)
21.    else
22.    Update the position of the coot by Eq. (5)
23.    end
24.    end
25.    Calculate the fitness of the coot
26.    if the fitness of coot < the fitness of leader (k)
27.    Temp=leader (k); leader (k)=coot; coot=Temp
28.    end
29.    end
30.    for the number of Leaders
31.    if rand < 0.5
32.    Update the position of the Leader by Eq. (10.1)
33.    else
34.    Update the position of the Leader by Eq. (10.2)
35.    end
36.    if the fitness of leader < gBest
37.    Temp=gBest; gBest=leader; leader=Temp; (Update Global optimum)
38.    end
39.    end
40. Iter = Iter + 1
41. end

```

$$\text{leaderpos}(i) = \begin{cases} B \times R_3 \times \cos(2R\pi) \times (g_{Best} - \text{leaderpos}(i)) \\ \quad + g_{Best} & R_4 < 0.5 \\ B \times R_3 \times \cos(2R\pi) \times (g_{Best} - \text{leaderpos}(i)) \\ \quad - g_{Best} & R_4 \geq 0.5 \end{cases} \quad (10)$$

g_{Best} : The best position ever found
 R_3 and R_4 : Random numbers in the interval [0, 1]
 B is calculated by Eq. (11)
 $B = 2 - L \times (1/Iter)$

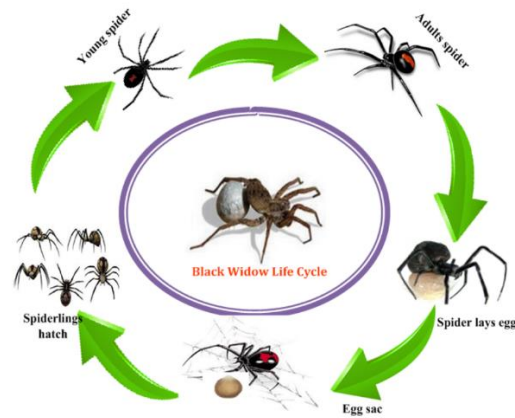


Fig. 10 Black Widow Spider's Life Cycle

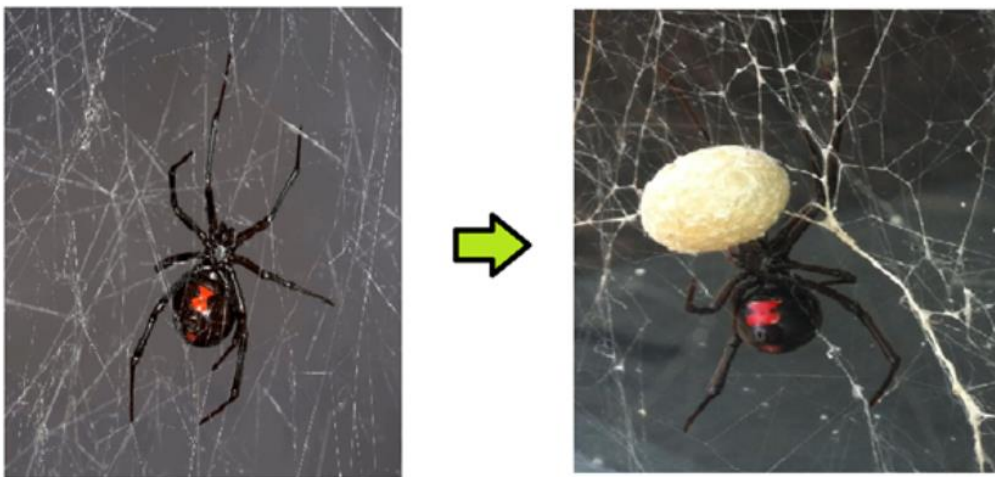


Fig. 11 (a) Female Black Widow on Her Web and (b) Female Black Widow with Her Egg Sac on Her Web

3.1.2 Black widow optimization algorithm (BWOA)

Hayyolalam and Kazem first presented the black widow optimization algorithm (*BWOA*), a brand-new meta-heuristic optimizer based on population, to address single target and continual optimization issues (Hayyolalam and Kazem 2020). The *BWOA* begins with a starting population made up of black widow spiders (i.e., particulars), and every spider indicates a potential answer to an optimization issue (Figs. 10-12). This is similar to various meta-heuristic algorithms based on population. The *BWOA* splits the development procedure into three stages, namely procreation, cannibalism, and mutation. This division of the evolution procedure is inspired by the black widow spiders' distinctive mating behavior and their peculiar qualities in procreating novel generations.

The *BWOA* calculates the appropriate number of participants in procreation during the reproduction stage using a procreation rate (*PP*), and therefore several pairs of parents are chosen randomly to engage in the reproduction operation to generate the next generation.

Three cannibalism strategies are used during the cannibalism stage. First, the female spider consumes the male one in a process known as sexual cannibalism. The target function values are used to distinguish between the

male and female spiders, with the female being considered to be the superior specimen. The second method, or cannibalism rate (*CR*), involves sibling cannibalism, which is carried out with a specified possibility. It means that the superior generation will consume the inferior one. The third technique seeks to explain a circumstance in which young spiders consume their parents. The third technique seeks to explain a circumstance in which young spiders consume their parents.

By modifying their features with a certain possibility, or mutation rate (*MP*), black widow spiders adapt to their natural habitat during the mutation stage. The goal of the mutation stage is to increase population variety, and the answer's structure is altered randomly. Once a specified stopping condition is met, the three previously indicated stages (i.e., searching operators) are repeated. The following sections list the key elements of a typical *BWOA*.

Population initialization

The progeny is created using Eq. (12) during the procreation stage, where α is an arrangement of randomly generated values from the range $[0, 1]$, ω_1 and ω_2 are two spider parent particulars, and ω'_1 and ω'_2 are two freshly created particulars. We may create n novel people by

Algorithm 2 Pseudo-code of *BWOA* (Hayyolalam and Kazem 2020)**Inputs:**

- ✚ Maximum number of iterations
- ✚ Rate of procreating
- ✚ Rate of cannibalism
- ✚ Rate of mutation

Output: Near-optimal solution for the objective function

1. ✦ Initialization
2. The initial population of black widow spiders
3. Each pop is a D-dimensional array of chromosomes for a D-dimensional problem
4. ✦ Loop until the terminal condition
5. Based on procreating rate, calculate the number of reproductions n_r
6. Select the best n_r solutions in pop and save them in pop
7. ✦ Procreating and cannibalism
8. **for** $i = 1: n_r$
9. Randomly select two solutions as parents from pop 1
10. Generate D children using Eq. (12)
11. Destroy father
12. Based on the cannibalism rate, destroy some of the children (new achieved solutions)
13. Save the remain solutions into pop 2
14. **end for**
15. ✦ Mutation
16. Based on the mutation rate, calculate the number of mutation children n_m
17. **for** $i = 1: n_m$ **do**
18. Select a solution from pop 1
19. Mutate randomly one chromosome of the solution and generate a new solution
20. Save the new one into pop 3
21. **end for**
22. ✦ Updating
23. Update $\text{pop} = \text{pop 2} + \text{pop 3}$
24. Returning the best solution
25. Return the best solution from pop



Fig. 12 Baby spiders leave their Egg Sac

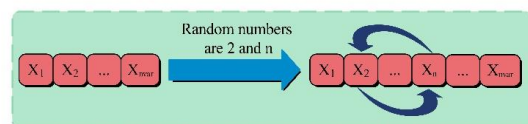


Fig. 13 Mutation

redoing Eq. (12) $n/2$ times, as seen below

$$\begin{aligned}\omega'_1 &= \alpha \times \omega_1 + (1 - \alpha) \times \omega_2 \\ \omega'_2 &= \alpha \times \omega_2 + (1 - \alpha) \times \omega_1\end{aligned}\quad (12)$$

Cannibalism stage

During the cannibalism stage, superior participants from the freshly formed population are chosen and stored through

sexual cannibalism, sibling cannibalism, and specific cannibalism.

Mutation phase

To improve the *BWOA*'s search capabilities, the mutation stage tries to increase population variety (Fig. 13). To do this, a specific mutation technique is used with a possibility *MP* above a selection of individuals. The pseudo-code and flowchart of *BWOA* are provided in Algorithm 2 and Fig. 14.

3.2 Applied analysis**3.2.1 Support vector regression (SVR)**

A supervised machine learning method that contains two kinds of presentation, for Classification and Regression, is known as Support vector regression. For time sequence analysis, *SVR* is confirmed to improve. The input data's dimensionality does not affect the calculational intricacy, which is the main advantage of utilizing the *SVR*. For forecast usages, *SVR* prevails over the Neural Networks' faults. Su *et al.* suggest an additive Support vector regression methodology which performs better than a Back diffusion neural network (Su *et al.* 2007).

The *SVR* variables' choice is a fundamental part that specifies the forecast's precision while using the time sequence analysis utilizing support vector regression. The following formula shows the traffic flow data utilized for training data collection.

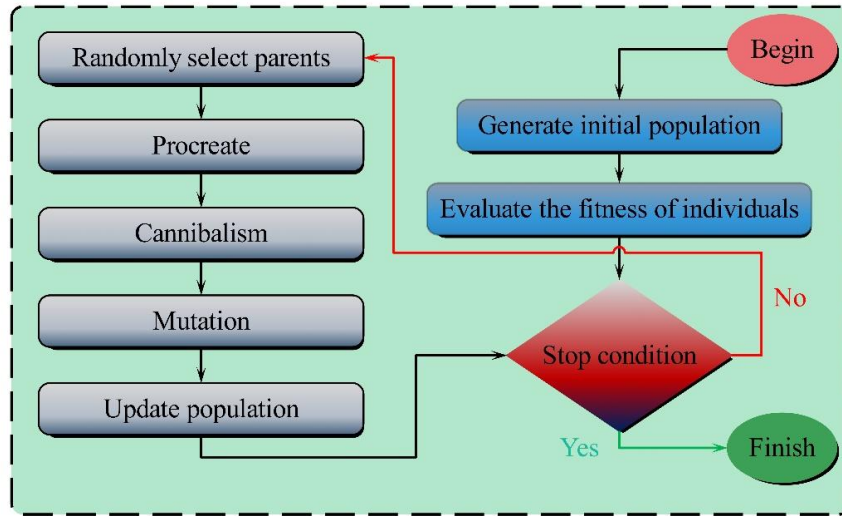


Fig. 14 Flowchart of BWOA

$$S = \{(x_k, y_k)\}_{k=1,2,3,\dots,P} \quad (13)$$

In this equation, P shows the training data samples' number. y_k and x_k are created in a multi-dimensional area as below

$$f(x) = W\phi_x + b \quad (14)$$

Based on the equation above, the training data is mapped by the bias value b , the weight vector w , and a nonlinear function ϕ_x . The target function (F)'s minimization is able to appraise the bias vector (b) and weight vector (w).

$$F = \frac{1}{2}W^2 + C \frac{1}{N} \sum_{k=1}^P L_\varepsilon(y_k, f(x_k)) \quad (15)$$

Where y_k recognizes as the main value, $f(x_k)$ shows the forecasted or appraised value, C stands for a constant and L_ε shows as training fault's measure, which is called ε -insensitive loss function.

$$L_\varepsilon = \begin{cases} |f(x) - y| - \varepsilon & \text{if } |f(x) - y| \geq \varepsilon \\ 0 & \text{otherwise} \end{cases} \quad (16)$$

Our suggested work's main target is to decrease the training fault.

$$\min \frac{1}{2}w^2 + C \sum_{k=1}^P (\beta + \bar{\beta}) \quad (17)$$

$$\text{Such that } \begin{cases} y_k - f(x_k) \leq \beta + \bar{\beta} \\ f(x_k) - y_k \leq \beta + \bar{\beta} \\ \bar{\beta} \geq 0, \beta \geq 0, k = 1, 2, 3, \dots, P \end{cases}$$

The non-negative parameters which denote the forecasted value's deflection and fundamental data samples are called β and $\bar{\beta}$. The forecast function is able to be presented below, utilizing Karush Kuhn Tucker's situation.

$$f(x) = \sum_{k=1}^P (a_k, a_k^*) K(x, x_k) \quad (18)$$

Such that $0 \leq a_k^* \leq C$

$$0 \leq a_k \leq C$$

a_k^* , and a_k are the Lagrange multipliers.

A function which maps nonlinear data to its linear form is the kernel function. Every function which pleases the situation of Mercer is able to operate as a kernel function. Hither kernel function $K(x, x_k)$ is described by the familiar Radial Bias function as follows with a parameter γ .

$$K(x, x_k) = \exp\left(-\frac{x - x_k}{2\gamma^2}\right) \quad (19)$$

The variables C , ε , γ have an influence on the predicting's precision in SVR. Fig. 15 defines the one-dimensional SVR.

3.2.2 Random Forests analysis (RF)

To address problems with classification, unsupervised learning, and regression, Breiman developed the RF technique (Breiman 2001, Liaw and Wiener 2002). This strategy has been successfully utilized in several contexts with positive results (Nhu *et al.* 2020). The RF methodology is superior to many other methods in a number of crucial ways, notably high precision and thorough data recorders with minimal gradation and parameters. The bagging strategy is employed to selectively select feature alternatives for system gradation in classification case problems from the whole collection of data (Ge *et al.* 2022). An Out-of-Bag (OOB) item was produced throughout the research coupled with two different kinds of errors: To score and select parameters, one may utilize a loss in accuracy and a decrease in Gini (Eq. (20)) (Archer and Kimes 2008, Scornet *et al.* 2015). When the variable quantities are changed due to OOB data, the function assesses the design defects for each parameter.

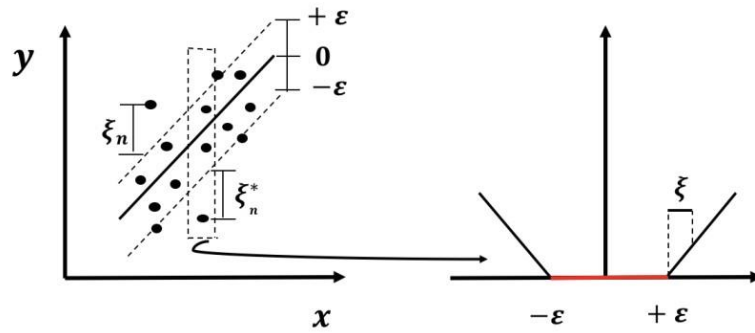


Fig. 15 A 1D linear SVR with an intense bandwidth (Smola and Schölkopf 2004)

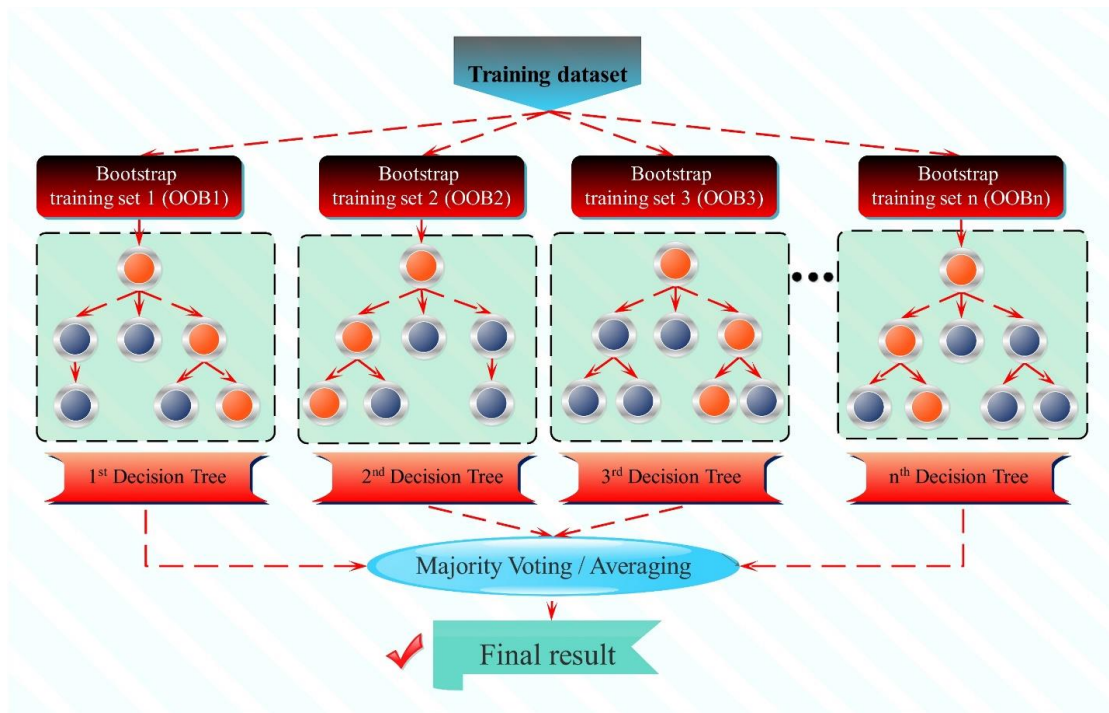


Fig. 16 RF model's creation flowchart (Breiman 2001, Liaw and Wiener 2002)

Fig. 16 depicts the steps involved in producing an RF.

$$GI(t_{X(x_i)}) = 1 - \sum_{j=1}^m f(t_{X(x_i),j})^2 \quad (20)$$

The *COM* and *BWOA* metaheuristic optimization algorithms were used to fine-tune the five critical RF architectural hyperparameters, which are crucial to the learning process. Table 2 displays the pertinent tuning hyperparameters and their meanings. For each set of parameters, eight RF versions were built to reduce the random splitting's unpredictability. All variable modifications of the optimization algorithms were created via a trial-and-error procedure. The training effectiveness from the 10-fold cross-validation was employed as an appropriate function of the *COM* and *BWOA* during the variables tuning phase. Within the optimization methods, each subset of the hyperparameters was represented by a particle. The locations that were changed to get the highest

Table 2 Pivotal hyperparameters specifying in RF (Qi et al. 2018)

Hyperparameters	Description
<i>MD*</i>	The highest depth of DTs
<i>MSS</i>	The lowest number of samples for the split
<i>MSL</i>	The lowest number of samples at the leaf node
<i>MDT</i>	The highest number of RT models in the ensemble
<i>MF</i>	The number of features selected during the choosing of the proper dividing

* $MD = Max_{Depth}$; $MSS = Min_{Samples_{Split}}$;

$MSL = Min_{Samples_{Leaf}}$; $MDT = Max_{DT}$; $MF = Max_{Features}$

fitness value, as well as the taken into consideration hyperparameters changed when the optimization processes were repeated. In the testing stage, the RF construction with the ideal hyperparameters was verified.

Table 3 Calculated performance criteria

Index	Quality	Formulation	Eq.
<i>Coefficient of determination</i>	Larger is good	$R^2 = \left(\frac{\sum_{s=1}^S (p_s - \bar{p})(z_s - \bar{t})}{\sqrt{[\sum_{s=1}^S (p_s - \bar{p})^2][\sum_{s=1}^S (z_s - \bar{t})^2]}} \right)^2$	(21)
<i>Root mean squared error</i>	Lower is good	$RMSE = \sqrt{\frac{1}{S} \sum_{s=1}^S (t_s - p_s)^2}$	(22)
<i>Relative Absolute Error</i>	Lower is good	$RAE = \frac{\sum_{s=1}^S p_s - t_s }{\sum_{s=1}^S p_s - \bar{p} }$	(23)
<i>Root Relative Squared Error</i>	Lower is good	$RRSE = \sqrt{\frac{\sum_{s=1}^S (p_s - t_s)^2}{\sum_{s=1}^S (p_s - \bar{p})^2}}$	(24)
<i>Mean absolute error</i>	Lower is good	$MAE = \frac{1}{S} \sum_{s=1}^S t_s - p_s $	(25)
<i>Performance index</i>	Lower is good	$PI = \frac{1}{\bar{p}} \frac{RMSE}{\sqrt{R^2 + 1}}$	(26)
<i>Variance account factor</i>	Larger is good	$VAF = \left(1 - \frac{var(p_s - t_s)}{var(p_s)} \right) * 100$	(27)
<i>A_{10-Index}</i>	Larger is good	$A_{10-Index} = \frac{S_{10}}{S}$	(28)
Uncertainty with a 95% confidence level (<i>U₉₅</i>) (Behar <i>et al.</i> 2015, Gueymard 2014)	Lower is good	$U_{95} = 1.96\sqrt{(SD^2 + RMSE^2)}$	(29)

Term:

- p_s and \bar{p} : The observations and average of them
- t_s and \bar{t} : The simulations and average of them
- S : The total number of data
- S_{10} : The specimens' number with a rate of records per simulated one in the interval of 0.9 and 1.1
- SD : Standard deviation

3.3 Workability metrics

One of the most important stages in the modeling process is the confirmation and evaluation of the given model. It's crucial to admit that the simulations have given accurate, adequate results for the set objectives once they have been created. In this study, eight modeling performance statistical criteria were used to evaluate the exactness and accuracy of the methodologies (Table 3).

4. Development, analysis, and discussion

As was already indicated, the major goal of the article was to offer new *RF* and *SVR* networks that could be integrated with various optimization techniques to estimate the settlement of a shallow foundation. Additionally, it was suggested that the most appropriate (optimal) values of the *SVR* determinative parameters (i.e., γ , C , and ϵ) and *RF* determinative components (*MD*, *MSS*, *MSL*, *MDT*, and *MF*) should be identified, where *COM* and *BWOA* approaches were used for this goal. Table 4 lists the *RF* and *SVR* networks' parameters that were taken into consideration, as well as the optimum values that were indicated.

For the goal of estimating the S_m , the results of

recommended hybridization networks called *COM-SVR*, *COM-RF*, *BWOA-RF*, and *BWOA-SVR* were collated and analyzed as follows. The training and examining portions of the considered dataset were divided at random by 75 and 25%, respectively. Fig. 17 shows the correlation between the predicted and measured S_m in the logarithmic dimensions for the *COM-SVR*, *COM-RF*, *BWOA-RF*, and *BWOA-SVR*. Different buildability measures were calculated and evaluated in data mining studies to describe the resilience and dependability of built networks. To achieve this goal, a number of measures, including R^2 , *RMSE*, *RAE*, *RRSE*, *MAE*, *PI*, *VAF*, and A_{10-I} , were computed and compared in Table 5. Along with this, a score-based analysis was designed by assigning scores to models from 1 (weak value) to 4 (best value), and finally, the total summation score depicts the outperformed model. The correctness and thoroughness of simulations may also be improved by comparing the findings of one research with those of earlier studies in order to validate the models, where an appropriate comparison with the hybrid *ANFIS-PSO* system was attempted (Mohammed *et al.*, 2020).

The results indicate that all created systems accurately simulated the S_m , with an R^2 of better than 0.979 and 0.9765 for the train and test data phases, respectively. This

Table 4 Selected parameter context to evaluate the largest precision of the methods

Optimizer	Parameter	Value	Hybrid method	Parameter	Value	
<i>BWOA</i>	<i>procreate rate</i>	0.3	<i>BWOA – SVR</i>	<i>Kernel function</i>	<i>RBF</i>	
	<i>mutation rate</i>	0.5		γ	0.102	
	<i>Number of iterations</i>	300		<i>C</i>	49.367	
	<i>Number of runs</i>	30		ε	0.248	
				<i>BWOA– RF</i>	<i>MD</i>	17
					<i>MSS</i>	3
					<i>MSL</i>	1
					<i>MDT</i>	507
		<i>MF</i>	0.925			
<i>COM</i>	<i>R</i>	[-1, 1]	<i>COM – SVR</i>	<i>Kernel function</i>	<i>RBF</i>	
	<i>R₁</i>	[0, 1]		γ	0.1	
	<i>R₂</i>	[0, 1]		<i>C</i>	34.367	
	<i>Population size</i>	30		ε	0.2048	
	<i>Number of iterations</i>	300		<i>COM– RF</i>	<i>MD</i>	16
	<i>Number of runs</i>	30			<i>MSS</i>	3
					<i>MSL</i>	1
					<i>MDT</i>	652
		<i>MF</i>	0.847			

Table 5 The findings of produced regression networks and comparison with the literature

Model	R^2	<i>RMSE</i>	<i>RAE</i>	<i>RRSE</i>	<i>MAE</i>	<i>PI</i>	<i>VAF</i>	A_{10-1}	<i>Rank</i>
<i>Training data</i>									
<i>BWOA – RF</i>	0.9854	3.1354	0.1042	0.1234	1.6925	0.081	98.481	0.5493	
Rank score	2	2	2	2	2	2	2	2	16
<i>BWOA – SVR</i>	0.979	3.7598	0.1347	0.1479	2.1868	0.0973	97.8156	0.4718	
Rank score	1	1	1	1	1	1	1	1	8
<i>COM – SVR</i>	0.9924	2.2913	0.0558	0.0901	0.9059	0.0591	99.1943	0.7606	
Rank score	3	3	3	3	3	3	3	3	24
<i>COM – RF</i>	0.9945	1.9658	0.0391	0.0773	0.6355	0.0507	99.4079	0.8099	
Rank score	4	4	4	4	4	4	4	4	32
<i>ANFIS – PSO</i> (Mohammed <i>et al.</i> 2020)	0.9025	8.09							
<i>Testing data</i>									
<i>BWOA – RF</i>	0.9799	4.3075	0.0821	0.1462	1.6857	0.0921	97.8931	0.8085	
Rank score	2	2	2	2	2	2	2	2	16
<i>BWOA – SVR</i>	0.9765	4.6608	0.1019	0.1582	2.0942	0.0997	97.5379	0.6596	
Rank score	1	1	1	1	1	1	1	1	8
<i>COM – SVR</i>	0.9831	4.0496	0.0579	0.1375	1.1889	0.0865	98.1571	0.8723	
Rank score	3	3	3	3	3	3	3	3	24
<i>COM – RF</i>	0.993	2.7805	0.0322	0.0944	0.6609	0.0592	99.1501	0.9362	
Rank score	4	4	4	4	4	4	4	4	32
<i>ANFIS – PSO</i> (Mohammed <i>et al.</i> 2020)	0.739	14.10							

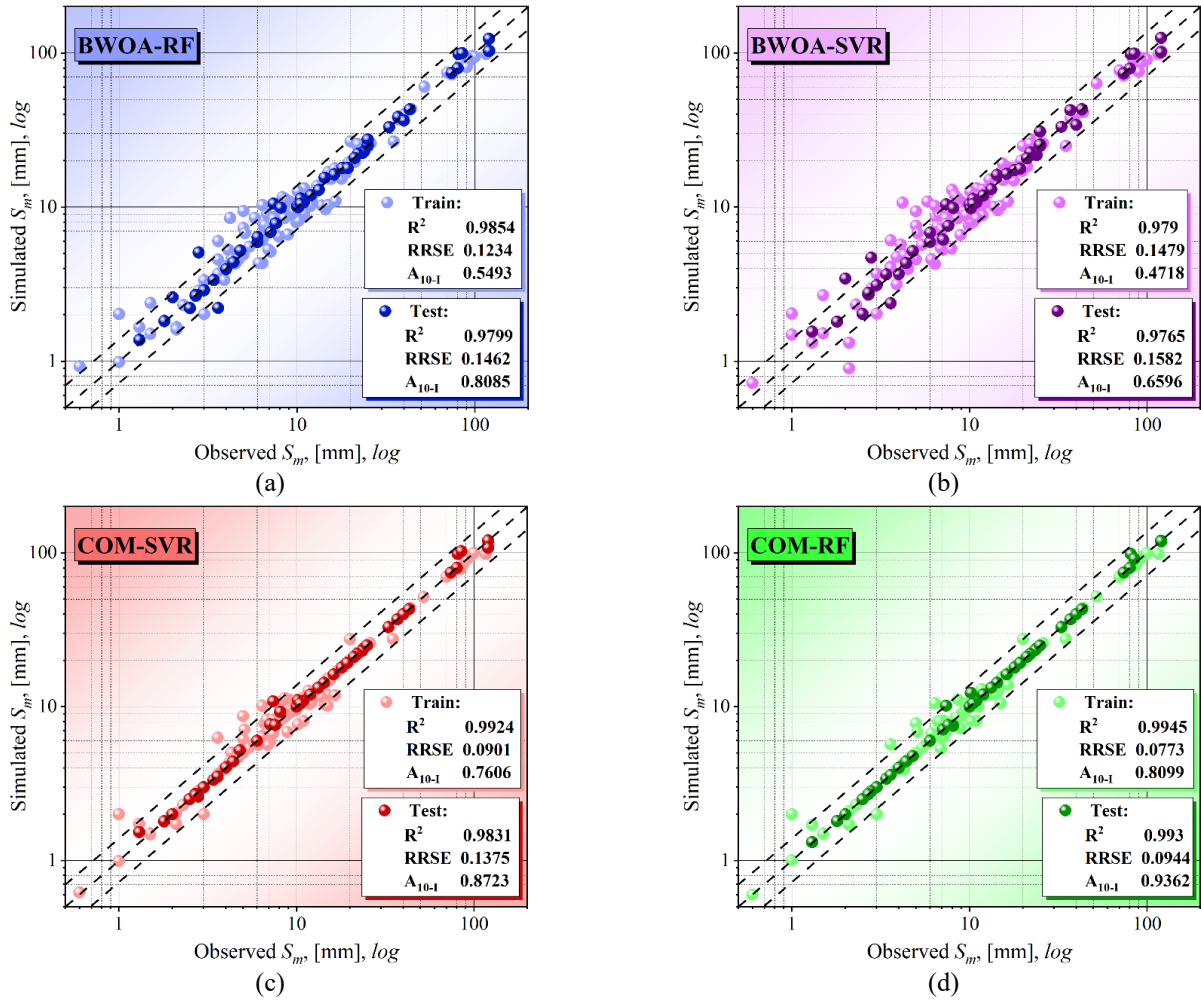
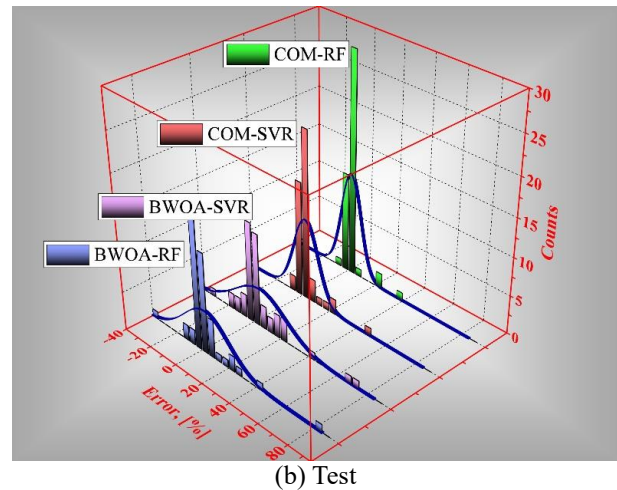
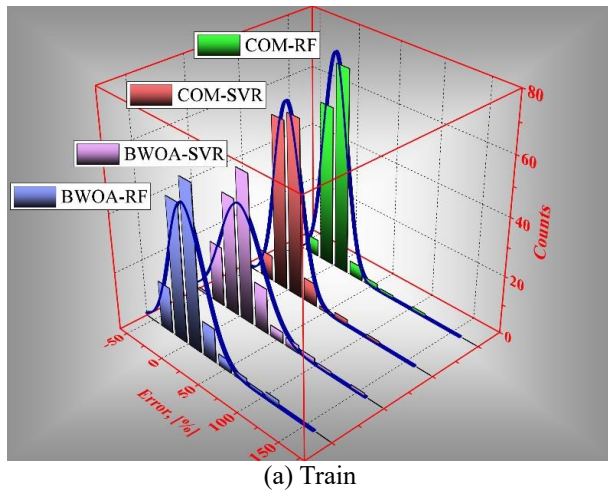
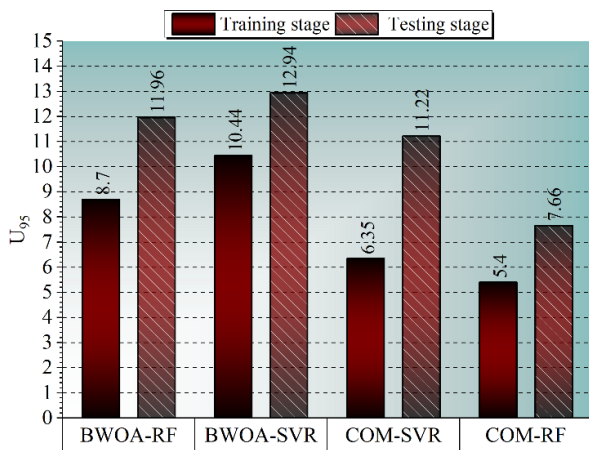


Fig. 17 The correlation scatter plot for S_m

indicates extraordinary efficiency and a good correlation between the experimental and simulated S_m . The advantage of $COM - RF$ over $BWOA - RF$, $BWOA - SVR$ and $COM - SVR$ is shown in considered two training and testing stages. In the training phase, the values of R^2 , VAF and A_{10-1} for $COM - RF$ are extremely better than other hybrid algorithms -the higher these values, the more reliable are-, with accounting for 0.9945, 99.40779, and 0.8099, respectively. $COM - SVR$ could gain the second-highest performance by receiving 0.9924, 99.1943, and 0.7606, respectively, higher than values related to $BWOA - RF$, followed by $BWOA - SVR$. Other indices which concentrated on the values of errors (i.e., $RMSE$, RAE , $RRSE$, MAE , and PI) also depicts the superiority of $COM - RF$ model respect to other hybrid ones, which depicts the powerfulness of RF machine learning method optimized with COM in the prediction procedure of S_m . Moreover, the exact trend is valid for the analysis with the testing dataset, with the powerfulness of $COM - RF$ model as confirmed by the aggregate ranking scores. When taking into account the two-phase outputs, the accumulated ranking scores show that $COM - RF$ could acquire a score of 32, followed by $COM - SVR$ with a score of 24, then $BWOA - RF$ at 16, and finally $BWOA - SVR$ with a score of 8.

As was previously mentioned, the literature produced by $ANFIS - PSO$ (Mohammed *et al.*, 2020) has been used to compare the results of this work. The model's results outperformed those of $ANFIS - PSO$ (Mohammed *et al.*, 2020), and $COM - RF$ findings were much outstanding to those of the literature. R^2 values rose from 0.9025 ($ANFIS - PSO$ (Mohammed *et al.*, 2020)) to 0.9945 (Train phase) and from 0.739 ($ANFIS - PSO$ (Mohammed *et al.*, 2020)) to 0.993 (Test phase). $RMSE$ values showed a significant decrease, reducing from 8.09 ($ANFIS - PSO$ (Mohammed *et al.* 2020)) to 1.9658 in the training stage, and from 14.10 ($ANFIS - PSO$ (Mohammed *et al.* 2020)) to 2.7805 in the testing portion. From the aforementioned justifications, as well as the information in Table 5 and Fig. 17, it can be concluded that, although other techniques were equally reliable in simulating the S_m of the shallow foundation, the suggested $COM - RF$ strategy excelled them all.

The dispersion of errors during the training and testing stages, where the result of the $COM - RF$, $COM - SVR$, $BWOA - RF$, and $BWOA - SVR$ frameworks is supplied, is shown in the plotted Fig. 18. The system's reliability rises as error distribution around the zero line, and shaper distribution curve grows. Due to its flattest distribution

Fig. 18 Error distribution of models in simulating S_m Fig. 19 The findings of U_{95} analysis

across both the training and testing, *BWOA-SVR* underperforms. The performance of *COM-RF* was better than *COM-SVR*, and it was followed by *BWOA-RF*, which had a sharper distribution throughout both the training and testing phases, along with its limited upper and lower bounds. As a result, when error distribution curves are considered, the *COM-RF* could be found to be the platform with the greatest performance, followed by the *COM-SVR*, *BWOA-RF*, and *BWOA-SVR*.

The values of U_{95} as robustness evaluators are shown in Fig. 19, where the generalization capacity rises as the uncertainty value falls. The *COM-RF* scenario specifically has the smallest levels of uncertainty when compared to other approaches, with $U_{95-Train}$ equal to 5.4 and $U_{95-Test}$ equal to 7.66, demonstrating its greater generalization capabilities. The second, third, and last ranks belonged to *COM-SVR* ($U_{95-Train}$ at 6.35, and $U_{95-Test}$ 11.22), *BWOA-RF* ($U_{95-Train}$ by 8.7, and $U_{95-Test}$ by 11.96), and *BWOA-SVR* ($U_{95-Train}$ at 10.44, and $U_{95-Test}$ 12.94) models, respectively. The descriptions and comparisons provide that *COM-RF* could carry out better than other frameworks.

This section includes a Taylor diagram (*TD*) to help you

more easily judge how well the recommended idea's function. Values for standard deviation (*SD*) are displayed on the *TD*'s vertical and horizontal axes, which are linked by red elliptical lines in Fig. 20. Wine lines represent the *RMSE* values, while red radial lines drawn from the coordinate origin represent the correlation coefficient (*R*). The data in this figure are intended to represent a benchmark with an *SD* value, *RMSE* of 0, and *R* equals 1. The performance of recommended methods, including *SD*, *RMSE*, and *R* is then evaluated in comparison to the reference record. In the training stage, the location of *COM-RF* is closer to the benchmark, with smaller superiority to *COM-SVR*. While *BWOA-RF* and *BWOA-SVR* located in the next performance rank, respectively. The same trend is also obvious for the testing stage; however, the performance of *COM-RF* as the outperformed model is clearer with respect to training data. After analyzing the *TD* data, it was possible to come to the conclusion that the *COM-RF* framework was better than others.

4.1 Limitations

This study uses artificial intelligence to evaluate the shallow foundation settling, which is affected by a number of factors. The kind and number of parameters are highly significant and useful when developing the framework of algorithms. These limits on future works may easily be addressed by expanding the amount of data from diverse projects, and it will also become more evident how adaptive the models built to analyses the shallow foundation settling are. A novel generation or direction of concepts that could be applied in many contexts is produced by the notion of employing new optimization approaches to enhance the output of computer models and artificial intelligence.

4.2 Sensitivity analysis

To determine the most important input variables to calculate the settlement, a sensitivity analysis of the models

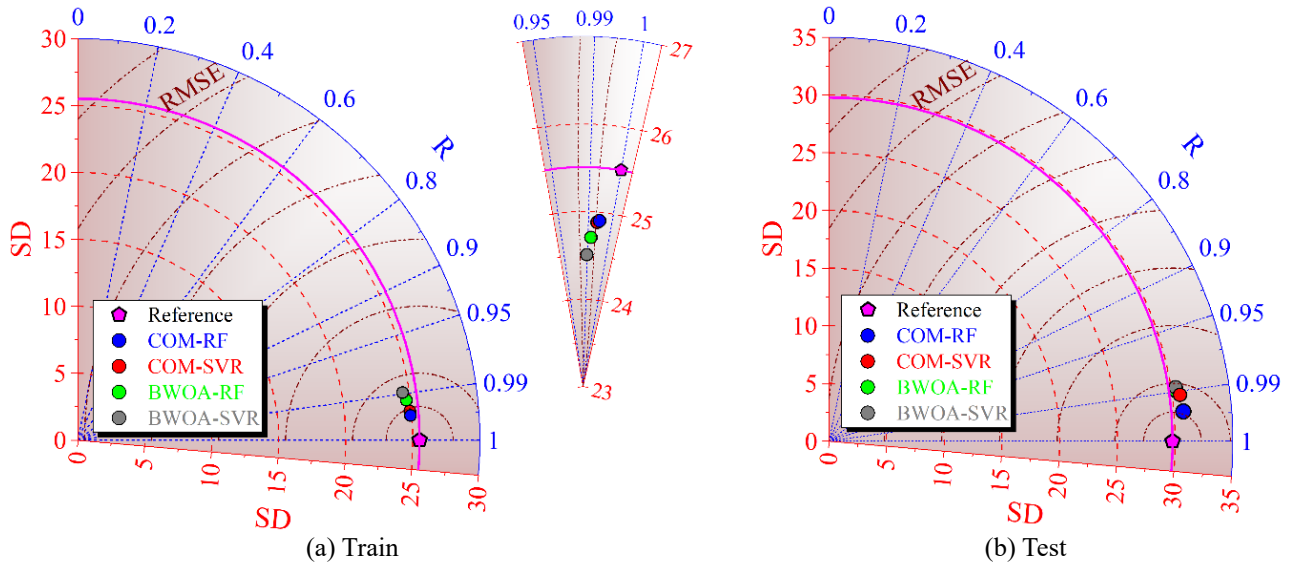


Fig. 20 Frameworks' performance comparison via Taylor diagram

Table 6 Sensitivity analysis by *COM – RF*

Inputs	Input parameters	RMSE	
		Train	Test
	–	1.9658	2.7805
$B,$	$q, N, D_f/H,$ and L/B	3.3245	4.0944
$q,$	$B, N, D_f/H,$ and L/B	2.9425	4.9059
$N,$	$B, q, D_f/H,$ and L/B	2.4056	4.3643
$D_f/H,$	$B, q, N,$ and L/B	3.4211	3.2101
and L/B	$B, q, N,$ and D_f/H	2.0849	3.0596

was performed. By concurrently eliminating one input parameter, different training data were created, and the test data set indicated the quantities of statistical performance index (*RMSE*). The statistical performance criteria are used to choose the ideal model for the sensitivity analysis. The *COM – RF* model was chosen for the current investigation because of its exceptional performance. The findings are presented in Table 7, which demonstrates that D_f/H , is the most important parameter for predicting settlement in the train phase, but q in the test phase. It is important to keep in mind that removing input variables may only result in a negligible performance loss for the model, but in the case of the current study, where the analysis was based on the findings of experimental measurements in order to pinpoint the effects of inputs on the settlement, doing so may reduce the model's generalizability. The current study does not favour eliminating any variables because the multicollinearity problem does not significantly affect a model's fit and frequently does not have a noticeable influence on predictions.

5. Conclusions

In the present study, the prediction of shallow

foundation settlement applying data mining methods was considered as the principal goal. Support Vector Regression (*SVR*) and Random Forests (*RF*) were considered because of their applicability and powerfulness. In this study, two newly developed optimization algorithms named the COOT optimization method (*COM*) and the black widow optimization algorithm (*BWOA*) were considered for finding the determinative variables of models. The accuracy and thoroughness of models may be improved by comparing the findings of one research with those of earlier studies in order to validate the models, where it was attempted to produce a reasonable comparison using the hybrid *ANFIS – PSO* model (Mohammed *et al.* 2020). The following are the key findings:

- The results indicate that all created systems accurately simulated the S_m , with an R^2 of better than 0.979 and 0.9765 for the train and test data phases, respectively. This indicates extraordinary efficiency and a good correlation between the experimental and simulated S_m .
- The advantage of *COM – RF* over *BWOA – RF*, *BWOA – SVR* and *COM – SVR* is shown in considered two training and testing stages. In the training phase, the values of R^2 , VAF and A_{10-1} for *COM – RF* were extremely better than other hybrid algorithms, accounting for 0.9945, 99.40779, and 0.8099, respectively. *COM – SVR* could gain the second-highest performance, higher than values related to *BWOA – RF*, followed by *BWOA – SVR*. Other indices which concentrated on the values of errors also depicted the superiority of *COM – RF* model with respect to other hybrid ones.
- The model's results outperformed those of *ANFIS – PSO* (Mohammed *et al.*, 2020), and *COM – RF* findings were much outstanding to those of the literature. R^2 values rose from 0.9025 (Mohammed *et al.* 2020) to 0.9945 (Train phase), and from 0.739 (Mohammed *et al.*, 2020) to 0.993 (Test phase). *RMSE* values showed a significant decrease.

- The *COM – RF* scenario specifically has the smallest levels of uncertainty when compared to other approaches, with $U_{95-Train}$ equal to 5.4 and $U_{95-Test}$ equal to 7.66, demonstrating its greater generalization capabilities. The second, third, and last ranks belonged to *COM – SVR*, *BWOA – RF*, and *BWOA – RF* models, respectively.
- The results of Taylor diagram analysis showed that, in the training stage, the location of *COM – RF* is closer to the benchmark, with smaller superiority to *COM – SVR*. While *BWOA – RF* and *BWOA – SVR* located in the next performance rank, respectively. The same trend was also obvious for the testing stage; however, the performance of *COM – RF* as the outperformed model is clearer with respect to training data.
- Finally, by analyzing established designs utilizing different analysis aspects, such as various error criteria, Taylor diagrams, uncertainty analyses, and error distribution, it was feasible to arrive at the final result that the recommended *COM – RF* was the outperformed approach in the forecasting process of S_m of shallow foundation, while other techniques were also reliable.

Acknowledgements

Survey of industrial land and establishment of database in Shengli East Road Area in Bengbu City of Anhui Province (880635); Domestic Visiting Project (gxgnfx2022042); Outstanding young and middle-aged backbone teachers project of college-level (210036); General Natural Science Project of College-level (2021zryb12).

References

- Aghayari Hir, M., Zaheri, M. and Rahimzadeh, N. (2022), "Prediction of rural travel demand by spatial regression and artificial neural network methods (Tabriz County)", *J. Transport. Res.*, <https://doi.org/10.22034/TRI.2022.312204.2970>.
- Al-Musawi, A.A., Alwanas, A.A.H., Salih, S.Q., Ali, Z.H., Tran, M.T. and Yaseen, Z.M. (2020), "Shear strength of SFRCB without stirrups simulation: implementation of hybrid artificial intelligence model", *Eng. with Comput.*, **36**(1), 1-11. <https://doi.org/10.1007/s00366-018-0681-8>.
- Alwanas, A.A.H., Al-Musawi, A.A., Salih, S.Q., Tao, H., Ali, M., and Yaseen, Z.M. (2019), "Load-carrying capacity and mode failure simulation of beam-column joint connection: Application of self-tuning machine learning model", *Eng. Struct.*, **194**, 220-229. <https://doi.org/10.1016/j.engstruct.2019.05.048>.
- Alzabeebee, S., Jamei, M., Hasanipناه, M., Amnieh, H.B., Karbasi, M. and Keawsawasvong, S. (2022), "Development of a new explicit soft computing model to predict the blast-induced ground vibration", *Geomech. Eng.*, **30**(6), 551-564. <https://doi.org/10.12989/gae.2022.30.6.551>.
- Archer, K.J. and Kimes, R.V. (2008), "Empirical characterization of random forest variable importance measures", *Comput. Stat. Data An.*, **52**(4), 2249-2260. <https://doi.org/10.1016/j.csda.2007.08.015>.
- Armaghani, D.J., Faradonbeh, R.S., Rezaei, H., Rashid, A.S.A., and Amnieh, H.B. (2018), "Settlement prediction of the rock-socketed piles through a new technique based on gene expression programming", *Neural Comput. Appl.*, **29**(11), 1115-1125. <https://doi.org/10.1007/s00521-016-2618-8>.
- Ashrafiyan, A., Shokri, F., Amiri, M.J.T., Yaseen, Z.M. and Rezaie-Balf, M. (2020), "Compressive strength of foamed cellular lightweight concrete simulation: New development of hybrid artificial intelligence model", *Constr. Build. Mater.*, **230**, 117048. <https://doi.org/10.1016/j.conbuildmat.2019.117048>.
- Babu, G.L.S. and Srivastava, A. (2007), "Reliability analysis of allowable pressure on shallow foundation using response surface method", *Comput. Geotech.*, **34**(3), 187-194. <https://doi.org/10.1016/j.compgeo.2006.11.002>.
- Behar, O., Khellaf, A. and Mohammedi, K. (2015), "Comparison of solar radiation models and their validation under Algerian climate-The case of direct irradiance", *Energ. Convers. Management*, **98**, 236-251. <https://doi.org/10.1016/j.enconman.2015.03.067>.
- Benemaran, R.S. and Esmacili-Falak, M. (2020a), "Optimization of cost and mechanical properties of concrete with admixtures using MARS and PSO", *Comput. Concrete*, **26**(4), 309-316. <https://doi.org/10.12989/cac.2020.26.4.309>.
- Breiman, L. (2001), "Random forests", *Machine Learning*, **45**(1), 5-32. <https://doi.org/10.1023/A:1010933404324>.
- Bungenstab, F.C. and Bicalho, K.V. (2016), "Settlement predictions of footings on sands using probabilistic analysis", *J. Rock Mech. Geotech. Eng.*, **8**(2), 198-203. <https://doi.org/10.1016/j.jrmge.2015.08.009>.
- Chen, H., Wu, L., Chen, J., Lu, W. and Ding, J. (2022), "A comparative study of automated legal text classification using random forests and deep learning", *Inform. Process. Management*, **59**(2), 102798. <https://doi.org/10.1016/j.ipm.2021.102798>.
- Chen, R.P., Zhang, P., Kang, X., Zhong, Z.Q., Liu, Y. and Wu, H.-N. (2019), "Prediction of maximum surface settlement caused by earth pressure balance (EPB) shield tunneling with ANN methods", *Soils Found.*, **59**(2), 284-295. <https://doi.org/10.1016/j.sandf.2018.11.005>.
- Chen, X.L., Fu, J.P., Yao, J.L. and Gan, J.F. (2018), "Prediction of shear strength for squat RC walls using a hybrid ANN-PSO model", *Eng. with Comput.*, **34**(2), 367-383. <https://doi.org/10.1007/s00366-017-0547-5>.
- Cherubini, C. (2000), "Reliability evaluation of shallow foundation bearing capacity on c'φ' soils", *Can. Geotech. J.*, **37**(1), 264-269.
- Consoli, N.C., Schnaid, F. and Milititsky, J. (1998), "Interpretation of plate load tests on residual soil site", *J. Geotech. Geoenviron. Eng.*, **124**(9), 857-867. [https://doi.org/10.1061/\(ASCE\)1090-0241\(1998\)124:9\(857\)](https://doi.org/10.1061/(ASCE)1090-0241(1998)124:9(857)).
- Dehghani, R., Babaali, H. and Zeydalinejad, N. (2022), "Evaluation of statistical models and modern hybrid artificial intelligence in the simulation of precipitation runoff process", *Sustain. Water Resour. Management*, **8**(5), 1-19. <https://doi.org/10.1007/s40899-022-00743-9>.
- Dehghani, R., Torabi Poudeh, H. and Izadi, Z. (2022), "Dissolved oxygen concentration predictions for running waters with using hybrid machine learning techniques", *Model. Earth Syst. Environ.*, **8**(2), 2599-2613. <https://doi.org/10.1007/s40808-021-01253-x>.
- Duncan, J.M. (2000), "Factors of safety and reliability in geotechnical engineering", *J. Geotech. Eng.*, **126**(4), 307-316.
- Easa, S.M. (1992), "Exact probabilistic solution of two-parameter bearing capacity for shallow foundations", *Can. Geotech. J.*, **29**(5), 867-870. <https://doi.org/10.1139/t92-094>.
- Esmacili-Choobar, N., Esmacili-Falak, M., Roohi-hir, M. and Keshtzad, S. (2013), "Evaluation of collapsibility potential at Talesh", *Iran. EJGE*, **18**, 2561-2573.

- Esmaili-Falak, M., Katebi, H. and Javadi, A. (2018), "Experimental study of the mechanical behavior of frozen soils- A case study of tabriz subway", *Periodica Polytechnica Civil Eng.*, **62**(1), 117-125. <https://doi.org/10.3311/PPci.10960>.
- Esmaili Falak, M. and Sarkhani Benemaran, R. (2022), "Investigating the stress-strain behavior of frozen clay using triaxial test", *J. Struct. Constr. Eng.*, [HTTSP://DOI.ORG/10.22065/JSCE.2022.332406.2747](https://doi.org/10.22065/JSCE.2022.332406.2747).
- Esmaili-Falak, M., Katebi, H., Vadiati, M. and Adamowski, J. (2019), "Predicting triaxial compressive strength and Young's modulus of frozen sand using artificial intelligence methods", *J. Cold Regions Eng.*, **33**(3), 04019007. [https://doi.org/10.1061/\(ASCE\)CR.1943-5495.0000188](https://doi.org/10.1061/(ASCE)CR.1943-5495.0000188).
- Farrar, D.E. and Glauber, R.R. (1967), "Multicollinearity in regression analysis: the problem revisited", *The Review of Economic and Statistics*, 92-107. <https://doi.org/10.2307/1937887>.
- Fattah, M.Y., Shlash, K.T. and Salim, N.M. (2013), "Prediction of settlement trough induced by tunneling in cohesive ground", *Acta Geotechnica*, **8**(2), 167-179. <https://doi.org/10.1007/s11440-012-0169-4>.
- Ge, D.M., Zhao, L.C. and Esmaili-Falak, M. (2022), "Estimation of rapid chloride permeability of SCC using hyperparameters optimized random forest models", *J. Sust. Cement-Based Mater.*, 1-19. <https://doi.org/10.1080/21650373.2022.2093291>.
- Ghosh, P., Neufeld, A. and Sahoo, J.K. (2022), "Forecasting directional movements of stock prices for intraday trading using LSTM and random forests", *Finance Res. Lett.*, **46**, 102280. <https://doi.org/10.1016/j.frl.2021.102280>.
- Gueymard, C.A. (2014), "A review of validation methodologies and statistical performance indicators for modeled solar radiation data: Towards a better bankability of solar projects", *Renew. Sust. Energ. Rev.*, **39**, 1024-1034. <https://doi.org/10.1016/j.rser.2014.07.117>.
- Hasanipanah, M., Noorian-Bidgoli, M., Jahed Armaghani, D. and Khamesi, H. (2016), "Feasibility of PSO-ANN model for predicting surface settlement caused by tunneling", *Eng. with Comput.*, **32**(4), 705-715. <https://doi.org/10.1007/s00366-016-0447-0>.
- Hayyolalam, V. and Kazem, A.A.P. (2020), "Black widow optimization algorithm: a novel meta-heuristic approach for solving engineering optimization problems", *Eng. Appl. Artif. Intell.*, **87**, 103249. <https://doi.org/10.1016/j.engappai.2019.103249>.
- Islam, M.M., Nagrial, M., Rizk, J. and Hellany, A. (2021), "Solar radiation and wind speed forecasting using deep learning technique", *Proceedings of the 2021 IEEE Asia-Pacific Conference on Computer Science and Data Engineering (CSDE)*, 1-6. <https://doi.org/10.1109/CSDE53843.2021.9718372>.
- Jebur, A.A., Atherton, W. and Al Khaddar, R. M. (2018), "Feasibility of an evolutionary artificial intelligence (AI) scheme for modelling of load settlement response of concrete piles embedded in cohesionless soil", *Ships Offshore Struct.*, **13**(7), 705-718. <https://doi.org/10.1080/17445302.2018.1447746>.
- Kamran, M., Shahani, N.M. and Armaghani, D.J. (2022), "Decision support system for underground coal pillar stability using unsupervised and supervised machine learning approaches", *Geomech. Eng.*, **30**(2), 107-121. [10.12989/gae.2022.30.2.107](https://doi.org/10.12989/gae.2022.30.2.107)
- Kar, A.K. (2016), "Bio inspired computing-a review of algorithms and scope of applications", *Exp. Syst. Appl.*, **59**, 20-32. <https://doi.org/10.1016/j.eswa.2016.04.018>.
- Karimi, I. (2003), "Application of Neuro-Fuzzy systems in estimating the response of sediment-filled valleys", *Proceedings of the 10th International Fuzzy Systems Association (IFSA) Congress*.
- Kidega, R., Ondiaka, M.N., Maina, D., Jonah, K.A.T. and Kamran, M. (2022), "Decision based uncertainty model to predict rockburst in underground engineering structures using gradient boosting algorithms", *Geomech. Eng.*, **30**(3), 259-272. <https://doi.org/10.12989/gae.2022.30.3.259>.
- Krizek, R.J., Corotis, R.B. and El-Moursi, H.H. (1978), "Probabilistic analysis of predicted and measured settlements: Can Geotech J, V14, N1, Feb 1977, P17-33", *Int. J. Rock Mech. Min. Sci. Geomech. Abstracts*, **15**(2), 28. <https://doi.org/10.1139/t77-002>
- Lehane, B. and Cosgrove, E. (2000), "Applying triaxial compression stiffness data to settlement prediction of shallow foundations on cohesionless soil", *Proceedings of the Institution of Civil Engineers-Geotechnical Engineering*, **143**(4), 191-200. <https://doi.org/10.1680/geng.2000.143.4.191>.
- Liaw, A. and Wiener, M. (2002), "Classification and regression by randomForest", *R News*, **2**(3), 18-22.
- Luo, J., Wu, C., Liu, X., Mi, D., Zeng, F. and Zeng, Y. (2018), "Prediction of soft soil foundation settlement in Guangxi granite area based on fuzzy neural network model", *Proceedings of the IOP Conference Series: Earth and Environmental Science*, **108**(3), 32034.
- Mahmoodzadeh, A., Nejati, H.R., Mohammadi, M., Ibrahim, H. H., Rashidi, S. and Mohammed, A.H. (2022), "Meta-heuristic optimization algorithms for prediction of fly-rock in the blasting operation of open-pit mines", *Geomech. Eng.*, **30**(6), 486-502. <https://doi.org/10.12989/gae.2022.30.6.489>.
- Maugeri, M., Castelli, F., Massimino, M.R. and Verona, G. (1998), "Observed and computed settlements of two shallow foundations on sand", *J. Geotech. Geoenviron. Eng.*, **124**(7), 595-605.
- Mayne, P.W. (2007), "In-situ test calibrations for evaluating soil parameters", *Characterization and Engineering Properties of Natural Soils, Vol. 3*. Taylor and Francis Group, London.
- Memar, S., Mahdavi-Meymand, A. and Sulisz, W. (2021), "Prediction of seasonal maximum wave height for unevenly spaced time series by Black Widow Optimization algorithm", *Mar. Struct.*, **78**, 103005. <https://doi.org/10.1016/j.marstruc.2021.103005>.
- Mirzaeiabdolyousefi, M., Mahmoodzadeh, A., Ibrahim, H.H., Rashidi, S., Majeed, M.K. and Mohammed, A.H. (2022), "Prediction of squeezing phenomenon in tunneling projects: Application of Gaussian process regression", *Geomech. Eng.*, **30**(1), 11-26. <https://doi.org/10.12989/gae.2022.30.1.011>.
- Mirzania, E., Kashani, M.H., Golmohammadi, G., Ibrahim, O.R. and Saroughi, M. (2022), *Hybrid COOT-ANN: a novel optimization algorithm for prediction of daily reference evapotranspiration in Australia*.
- Moayedi, H. and Jahed Armaghani, D. (2018), "Optimizing an ANN model with ICA for estimating bearing capacity of driven pile in cohesionless soil", *Eng. with Comput.*, **34**(2), 347-356. <https://doi.org/10.1007/s00366-017-0545-7>.
- Mohammed, M., Sharafati, A., Al-Ansari, N. and Yaseen, Z.M. (2020), "Shallow foundation settlement quantification: application of hybridized adaptive neuro-fuzzy inference system model", *Adv. Civil Eng.*, 2020. <https://doi.org/10.1155/2020/7381617>.
- Naderpour, H., Mirrashid, M. and Nagai, K. (2020), "An innovative approach for bond strength modeling in FRP strip-to-concrete joints using adaptive neuro-fuzzy inference system", *Eng. with Comput.*, **36**(3), 1083-1100. <https://doi.org/10.1007/s00366-019-00751-y>.
- Naderpour, H., Nagai, K., Haji, M. and Mirrashid, M. (2019), "Adaptive neuro-fuzzy inference modelling and sensitivity analysis for capacity estimation of fiber reinforced polymer-strengthened circular reinforced concrete columns", *Exp. Syst.*

- 36(4), e12410. <https://doi.org/10.1111/exsy.12410>.
- Naruei, I. and Keynia, F. (2021), "A new optimization method based on COOT bird natural life model", *Exp. Syst. Appl.*, **183**, 115352. <https://doi.org/10.1016/j.eswa.2021.115352>.
- Nhu, V.H., Hoang, N.D., Duong, V.B., Vu, H.D. and Bui, D.T. (2020), "A hybrid computational intelligence approach for predicting soil shear strength for urban housing construction: a case study at Vinhomes Imperia project, Hai Phong city (Vietnam)", *Eng. with Comput.*, **36**(2), 603-616. <https://doi.org/10.1007/s00366-019-00718-z>.
- Peschl, G.M., Schweiger, H., Pöttler, R. and Thurner, R. (2002), "Reliability analysis in geotechnics with deterministic finite elements—a simplified approach for practical application in tunnelling", *Proceedings of the International Conference on Probabilistics in Geotechnics—Technical and Economic Risk Estimation*, 121-128.
- Pham, B.T., Nguyen, M.D., Bui, K.T.T., Prakash, I., Chapi, K. and Bui, D.T. (2019), "A novel artificial intelligence approach based on multi-layer perceptron neural network and biogeography-based optimization for predicting coefficient of consolidation of soil", *Catena*, **173**, 302-311. <https://doi.org/10.1016/j.catena.2018.10.004>.
- Phoon, K.K. (2002), "Potential application of reliability-based design to geotechnical engineering", *Proceedings of the 4th Colombian Geotechnical Seminar*, 1-24.
- Qi, C., Chen, Q., Fourie, A. and Zhang, Q. (2018), "An intelligent modelling framework for mechanical properties of cemented paste backfill", *Min. Eng.*, **123**, 16-27. <https://doi.org/10.1016/j.mineng.2018.04.010>.
- Robertson, P.K. and Cabal, K.L. (2014), "Guide to cone penetration testing for geotechnical engineering", *California: Gregg Drilling and Testing. Inc.*
- Samui, P. (2008), "Support vector machine applied to settlement of shallow foundations on cohesionless soils", *Comput. Geotech.*, **35**(3), 419-427. <https://doi.org/10.1016/j.compgeo.2007.06.014>.
- Samui, P. and Sitharam, T.G. (2008), "Least-square support vector machine applied to settlement of shallow foundations on cohesionless soils", *Int. J. Numer. Anal. Method. Geomech.*, **32**(17), 2033-2043. <https://doi.org/10.1002/nag.731>.
- Sarkhani Benemaran, R., Esmacili-Falak, M. and Javadi, A. (2022), "Predicting resilient modulus of flexible pavement foundation using extreme gradient boosting based optimised models", *Int. J. Pavement Eng.*, 1-20. <https://doi.org/10.1080/10298436.2022.2095385>.
- Sarkhani Benemaran, R., Esmacili-Falak, M. and Katebi, H. (2020), "Physical and numerical modelling of pile-stabilised saturated layered slopes", *Proceedings of the Institution of Civil Engineers-Geotechnical Engineering*, 1-16. <https://doi.org/https://doi.org/10.1680/jgeen.20.00152>.
- Schmertmann, J.H. (1970), "Static cone to compute static settlement over sand", *J. Soil Mech. Found. Div.*, **96**(3), 1011-1043. <https://doi.org/10.1061/JSFEAQ.0001418>.
- Scornet, E., Biau, G. and Vert, J.P. (2015), "Consistency of random forests", *The Annals of Statistics*, **43**(4), 1716-1741.
- Shahin, M.A., Maier, H.R. and Jaksa, M.B. (2003a), "Settlement prediction of shallow foundations on granular soils using B-spline neurofuzzy models", *Comput. Geotech.*, **30**(8), 637-647. <https://doi.org/10.1016/j.compgeo.2003.09.004>.
- Shahin, M.A., Maier, H.R. and Jaksa, M.B. (2003b), "Neural and neurofuzzy techniques applied to modelling settlement of shallow foundations on granular soils", *Proceedings of the Int. Congress on Modeling and Simulation, MODSIM2003*, **4**, 1886-1891.
- Shahin, Mohamed A, Jaksa, M.B. and Maier, H.R. (2001), "Artificial neural network applications in geotechnical engineering", *Australian Geomech.*, **36**(1), 49-62.
- Shahin, Mohamed Amin (2003), "Use of artificial neural networks for predicting settlement of shallow foundations on cohesionless soils/Mohamed A. Shahin".
- Sharafati, A., Haghbin, M., Motta, D. and Yaseen, Z.M. (2021), "The application of soft computing models and empirical formulations for hydraulic structure scouring depth simulation: a comprehensive review, assessment and possible future research direction", *Arch. Comput. Method. Eng.*, **28**(2), 423-447. <https://doi.org/10.1007/s11831-019-09382-4>.
- Shi, J., Ortigao, J.A.R. and Bai, J. (1998), "Modular neural networks for predicting settlements during tunneling", *J. Geotech. Geoenviron. Eng.*, **124**(5), 389-395.
- Shi, X., Yu, X. and Esmacili-Falak, M. (2023), "Improved arithmetic optimization algorithm and its application to carbon fiber reinforced polymer-steel bond strength estimation", *Compos. Struct.*, **306**, 116599.
- Sivakugan, N., Eckersley, J. and Li, H. (1998), "Settlement predictions using neural networks", *Australian Civil Eng. Transactions*, **40**, 49-52.
- Smola, A.J. and Schölkopf, B. (2004), "A tutorial on support vector regression, statist", *Comput.*, **14**, 199-222. <https://doi.org/10.1023/B:STCO.0000035301.49549.88>.
- Soleimani, S., Jiao, P., Rajaei, S. and Forsati, R. (2018), "A new approach for prediction of collapse settlement of sandy gravel soils", *Eng. with Comput.*, **34**(1), 15-24. <https://doi.org/10.1007/s00366-017-0517-y>.
- Standard, A. (2008), "Standard test method for standard penetration test (SPT) and split-barrel sampling of soils".
- Su, H., Zhang, L. and Yu, S. (2007), "Short-term traffic flow prediction based on incremental support vector regression", *Proceedings of the 3rd International Conference on Natural Computation (ICNC 2007)*, **1**, 640-645. <https://doi.org/10.1109/ICNC.2007.661>.
- Tarawneh, B. (2017), "Predicting standard penetration test N-value from cone penetration test data using artificial neural networks", *Geosci. Front.*, **8**(1), 199-204.
- Tarawneh, B., Masada, T. and Sargand, S. (2013), "Estimated and measured settlements of shallow foundation supporting bridge substructure", *Jordan J. Civil Eng.*, **7**(2), 224-235.
- Teh, C.I., Wong, K.S., Goh, A.T.C. and Jaritngam, S. (1997), "Prediction of pile capacity using neural networks", *J. Comput. Civil Eng.*, **11**(2), 129-138. [https://doi.org/10.1061/\(ASCE\)0887-3801\(1997\)11:2\(129\)](https://doi.org/10.1061/(ASCE)0887-3801(1997)11:2(129)).
- Trenchard, H. (2012), "American coot collective on-water dynamics", *ArXiv Preprint ArXiv:1205.5929*.
- Tsai, H.C., Tyan, Y.Y., Wu, Y.W. and Lin, Y.H. (2013), "Determining ultimate bearing capacity of shallow foundations using a genetic programming system", *Neural Comput. Appl.*, **23**(7), 2073-2084. <https://doi.org/10.1007/s00521-012-1150-8>.
- Wang, L., Wu, C., Gu, X., Liu, H., Mei, G. and Zhang, W. (2020), "Probabilistic stability analysis of earth dam slope under transient seepage using multivariate adaptive regression splines", *Bull. Eng. Geol. Environ.*, **79**(6), 2763-2775. <https://doi.org/10.1007/s10064-020-01730-0>.
- Whitman, R.V. (2000), "Organizing and evaluating uncertainty in geotechnical engineering", *J. Geotech. Eng.*, **126**(7), 583-593.
- Yaseen, Z.M., Afan, H.A. and Tran, M.T. (2018), "Beam-column joint shear prediction using hybridized deep learning neural network with genetic algorithm", *Proceedings of the IOP Conference Series: Earth and Environmental Science*, **143**(1), 12025. <https://doi.org/10.1088/1755-1315/143/1/012025>.
- Yaseen, Z.M., Tran, M.T., Kim, S., Bakhshpoori, T. and Deo, R.C. (2018), "Shear strength prediction of steel fiber reinforced concrete beam using hybrid intelligence models: a new approach", *Eng. Struct.*, **177**, 244-255. <https://doi.org/10.1016/j.engstruct.2018.09.074>.
- Yang, C., Feng, H. and Esmacili-Falak, M. (2022), "Predicting the compressive strength of modified recycled aggregate concrete",

- Struct. Concrete*, **23**(6), 3696-3717.
<https://doi.org/10.1002/suco.202100681>.
- Yuan, J., Zhao, M. and Esmacili-Falak, M. (2022), "A comparative study on predicting the rapid chloride permeability of self-compacting concrete using meta-heuristic algorithm and artificial intelligence techniques", *Struct. Concrete*, **23**(2), 753-774. <https://doi.org/10.1002/suco.202100682>.
- Zhang, W. and Goh, A.T.C. (2012), "Reliability assessment on ultimate and serviceability limit states and determination of critical factor of safety for underground rock caverns", *Tunn. Undergr. Sp. Tech.*, **32**, 221-230.
<https://doi.org/10.1016/j.tust.2012.07.002>
- Zhu, W., Huang, L., Mao, L. and Esmacili-Falak, M. (2022), "Predicting the uniaxial compressive strength of oil palm shell lightweight aggregate concrete using artificial intelligence-based algorithms", *Struct. Concrete*, **23**(6), 3631-3650.
<https://doi.org/10.1002/suco.202100656>.

Notation

S_m	settlement of shallow foundations
SVR	support vector regression
RF	random forests
COM	coot optimization algorithm
$BWOA$	black widow optimization algorithm
MLP	Multi-layer perceptron
CPT	cone penetration test
ANN	Artificial neural network
B	footing width
q	footing net applied pressure
N	the average SPT blow count
D_f/H	footing embedment ration
L/B	footing geometry
R^2	Coefficient of determination
$RMSE$	Root mean squared error
RAE	Relative Absolute Error
$RRSE$	Root Relative Squared Error
MAE	Mean absolute error
PI	Performance index
VAF	Variance account factor
U_{95}	Uncertainty with a 95% confidence level
RBF	Radial basis function
$ANFIS$	Adaptive neuro-fuzzy inference system
PSO	Particle swarm optimization